J Membrane Biol (2015) 248:583–594
DOI 10.1007/s00232-014-9709-1

Calibration of Distribution Analysis of the Depth of Membrane Penetration Using Simulations and Depth-Dependent Fluorescence Quenching

Alexander Kyrychenko · Mykola V. Rodnin · Alexey S. Ladokhin

Received: 19 May 2014 / Accepted: 15 July 2014 / Published online: 9 August 2014

Abstract Determination of the depth of membrane penetration provides important information for studies of membrane protein folding and protein–lipid interactions. Here, we use a combination of molecular dynamics (MD) simulations and depth-dependent fluorescence quenching to calibrate the methodology for extracting quantitative information on membrane penetration. In order to investigate the immersion depth of the fluorescent label in lipid bilayer, we studied 7-nitrobenz-2-oxa-1,3-diazole (NBD) attached to the lipid headgroup in NBD-PE incorporated into POPC bilayer. The immersion depth of NBD was estimated by measuring steady-state and time-resolved fluorescence quenching with spin-labeled lipids co-incorporated into lipid vesicles. Six different spin-labeled lipids were utilized: one with headgroup-attached Tempo probe (Tempo-PC) and five with acyl chain-labeled *n*-Doxyl moieties (*n*-Doxyl-PC where *n* is a chain labeling position equal to 5, 7, 10, 12, and 14, respectively). The Stern–Volmer analysis revealed that NBD quenching in membranes occurs by both static and dynamic collisional quenching processes. Using the methodology of Distribution Analysis, the immersion depth and the apparent half-width of the transversal distributions of the NBD moiety were estimated to be 14.7 and 6.7 Å, respectively, from the bilayer center. This position is independently validated by atomistic MD simulations of NBD-PE lipids in a POPC bilayer (14.4 Å). In addition, we demonstrate that MD simulations of the transverse overlap integrals between dye and quencher distributions can be used for proper analysis of the depth-dependent quenching profile. Finally, we illustrate the application of this methodology by determining membrane penetration of site selectively labeled mutants of diphtheria toxin T-domain.

Keywords NBD-PE · Depth-dependent fluorescence quenching · Distribution analysis · Diphtheria toxin · Molecular dynamics simulations

Abbreviations

NBD-PE	1,2-dipalmitoyl-*sn*-glycero-3-phosphoethanolamine-*N*-(7-nitro-2-1,3-benzoxadiazol-4-yl)
Tempo-PC	1-Palmitoyl-2-oleoyl-*sn*-glycero-3-phospho(TEMPO)choline
n-Doxyl-PC	1-Palmitoyl-2-stearoyl-(*n*-Doxyl)-*sn*-glycero-3-phosphocholine
POPC	1-Palmitoyl-2-oleoyl-*sn*-glycero-3-phosphocholine
LUV	Large unilamellar lipid vesicle
FRET	Förster resonance energy transfer
MD simulation	Molecular dynamics simulation
DA	Distribution analysis
COM	Center of mass

Introduction

Site-selective labeling of proteins and peptides with various reporter groups is widely utilized in studies of membrane protein folding and lipid–protein interactions

A. Kyrychenko (✉)
Institute of Chemistry and School of Chemistry, V. N. Karazin Kharkiv National University, 4 Svobody Square, Kharkiv 61022, Ukraine
e-mail: a.v.kyrychenko@karazin.ua

A. Kyrychenko · M. V. Rodnin · A. S. Ladokhin
Department of Biochemistry and Molecular Biology, Kansas University Medical Center, Kansas City, KS 66160-7421, USA

(Kaback and Wu 1999). One of the methods that allows for quantitative determination of bilayer penetration is depth-dependent fluorescence quenching with lipid-attached quenchers (London and Ladokhin 2002). The principal method for extracting quantitative information on transverse distribution of the fluorophore is Distribution Analysis (DA), (Ladokhin 1997; London and Ladokhin 2002; Ladokhin 1999a, 2014) the main assumptions of which were recently validated in the context of pseudo-quenching analysis of MD simulation of a model tryptophan-containing compound (Kyrychenko et al. 2013). Here, we further validate the quantitative DA approach using experimental and computational approaches applied to the model lipid-attached fluorophore compound NBD-PE.

Among a variety of fluorescent lipids, NBD-functionalized phospholipids have been widely utilized as fluorescent analogs of native lipids to measure membrane polarity (Chattopadhyay and London 1988); (Chattopadhyay and Mukherjee 1999b), hydrogen bonding (Greiner et al. 2009), and lateral diffusion (Shrive et al. 1996) as well as lipid heterogeneity (Armstrong et al. 2003); (Pucadyil et al. 2007); (Vaish and Sanyal 2011). Lipids and cholesterol analogs labeled with an NBD fluorophore have also been used to detect the presence of lipid domains in cell membranes (Stubbs et al. 1989). NBD-labeled phospholipids have often been applied to determine the depth position of other fluorophores within membranes by FRET (Feigenson 1997); (Posokhov and Ladokhin 2006); (Loura 2012). Despite the broad application range of NBD-PE probe, a limited number of studies have attempted to characterize its structure in the membrane environment and the immersion depth of the NBD groups (Mazères et al. 1996). Fluorescence (Loura and Ramalho 2007) and NMR (Huster et al. 2003) experiments, as well as molecular dynamics (MD) simulations (Loura et al. 2008) have shown that when a polar NBD fluorophore was covalently attached to a fatty acyl chain, it could cause backfolding of the entire chain of the host lipid molecule toward the membrane interface (Loura and Prates Ramalho 2011). Therefore, it has been suggested that the location of an NBD group in a membrane often reflects its intrinsic properties rather than the nature and attachment positions in host lipids (Skaug et al. 2009); (Filipe et al. 2011).

In our recent studies, we have developed an integral approach for depth-dependent quenching of fluorophores in membranes based on a joint structural refinement using fluorescence measurements and MD simulations (Kyrychenko et al. 2010, 2011, 2013); (Kyrychenko and Ladokhin 2013). In this study, we used NBD-PE as a benchmark system for further development and calibration of a concerted approach, combining fluorescence experiments and MD simulations: In the experimental part, the immersion depth of the NBD fluorophore was estimated by depth-dependent fluorescence measurements of NBD-PE co-incorporated with Doxyl-labeled lipids (Doxyl-PC) located at graded depths within the membrane. The immersion depths of the spin probes were tuned by varying the attachment position of the spin group ranging from headgroup-labeled Tempo-PC to the acyl chain-labeled *n*-Doxyl-PCs. First, we measured steady-state and lifetime fluorescence quenching of the NBD label by the spin-labeled lipids. The NBD quenching profiles were found to be a smooth and predictable function of the attachment position and hence membrane depths of the spin probe in the corresponding labeled lipids. Our recent MD studies indicate that a nitroxide spin probe attached to specific positions along the acyl chain of phospholipids was not confined to fixed locations; it was free to span a broad range of depths within the bilayer (Kyrychenko et al. 2013). In this work, we used these MD-estimated depths of the spin probes to calculate the immersion depth of the NBD group by using the Distribution Analysis (DA) method (Ladokhin 1997, 1999a, b).

In the computational part, we carried out MD simulations of NBD-PE lipids inserted into an equilibrated POPC bilayer in water. Free, 160-ns long MD sampling allowed us to estimate the distribution profile of the NBD group within the membrane. This profile could be directly compared to that of the experimental quenching dependence approximated by the DA Gaussian profile. The MD-estimated depth of the NBD fluorophore was found to be in good agreement with the DA-calculated experimental depth, pointing to a promising role for a concerted spectroscopy/MD approach in predicting the structure of fluorescent lipids in a membrane. We illustrate the application of this approach by determining the depth of bilayer penetration of the P378C and N366C mutants of diphtheria toxin T-domain.

Materials and Methods

Materials

1-palmitoyl-2-oleoyl-*sn*-glycero-3-phosphocholine (POPC), 1-palmitoyl-2-stearoyl-(*n*–Doxyl)-*sn*-glycero-3-phosphocholine (*n*–Doxyl–PC), and 1-palmitoyl-2-oleoyl-*sn*-glycero-3-phospho(TEMPO)choline (Tempo-PC), and 1,2-dipalmitoyl-*sn*-glycero-3-phosphoethanolamine-*N*-(7-nitro-2-1,3-benzoxadiazol-4-yl) (NBD-PE) were obtained from Avanti Polar Lipids (Alabaster, AL). IANBD ester was from Invitrogen (Carlsbad, CA). To prepare samples for depth-dependent fluorescence measurements, NBD-PE, spin-labeled PCs, and unlabeled POPC lipids were first dissolved in chloroform solution and then dried under a high vacuum for ~12 h. The dried lipid mixtures were dissolved in 50 mM sodium

phosphate buffer, pH 8, and vortexed to disperse the lipids. Large unilamellar vesicles (LUV) of 0.1 μm diameter were prepared by extrusion (Mayer et al. 1986). Lipid concentrations of stock solutions were determined according to the procedure of Bartlett (1959).

Fluorescence Measurements

Fluorescence was measured using an SPEX Fluorolog FL3-22 steady-state fluorescence spectrometer (Jobin–Yvon, Edison, NJ) equipped with double-grating excitation and emission monochromators. The measurements were made in a 2 × 10 mm cuvette oriented perpendicular to the excitation beam and maintained at 25 °C using a Peltier device from Quantum Northwest (Spokane, WA). For NBD measurements, the excitation wavelength was 465 nm and the slits were 5 nm. Fluorescence decays were measured with a time-resolved fluorescence spectrometer, FluoTime 200 (PicoQuant, Berlin, Germany), using a standard time-correlated single-photon counting scheme (Posokhov and Ladokhin 2006). Samples were excited at 375 nm by a subnanosecond pulsed diode laser, LDH 375 (PicoQuant, Berlin, Germany), with a repetition rate of 10 MHz. Fluorescence emission was detected at 535 nm, selected by a Sciencetech Model 9030 monochromator, using a PMA-182 photomultiplier (PicoQuant, Berlin, Germany) (Kyrychenko et al. 2009). The fluorescence intensity decay was analyzed using FluoFit iterative-fitting software based on the Marquardt algorithm (PicoQuant, Berlin, Germany).

Preparation and Labeling of Single-Cys Mutants of T-domain

pET15b plasmid containing the diphtheria toxin T-domain gene with mutation C201S has been used as a template for mutagenesis. Introduction of point Cys mutations for specific labeling with NBD derivatives was performed by site-directed mutagenesis with the QuikChange site-directed mutagenesis kit from Stratagene (Cedar Creek, TX) and verified by DNA sequencing with T7 primer. Protein expression was performed in BL21 DE3pLys Escherichia coli cells, and recombinant protein synthesis was induced by the addition of 0.8 mM IPTG at $OD_{600} = 0.5$, after which cells were grown at 25 °C overnight. Purification included affinity chromatography on Ni–NTA resin from Qiagen (Valencia, CA) and gel filtration on a Sepharose 12, 1 × 30 cm column from GE Healthcare (Giles, U.K.), in PBS buffer containing 0.1 mM EDTA. The purity of preparations obtained was analyzed by SDS-PAGE. For determination of protein concentrations, we used a molar extinction coefficient of 17,000 M^{-1} cm^{-1} at 278 nm. Labeling with NBD dye was performed using a standard procedure for the thiol-reactive derivatives (Rodnin et al. 2008; Kyrychenko et al. 2009).

Molecular Dynamics Simulation Setup

NBD-PE lipids were studied in a 1-palmitoyl-2-oleoyl-phosphatidylcholine (POPC) bilayer. The initial configuration of an equilibrated POPC bilayer composed of 128 lipids was used from our previous studies (Kyrychenko 2010; Kyrychenko et al. 2010, 2011). In the initial system, 4 POPC lipid molecules were randomly selected for NBD labeling. The NBD labels were inserted into the equilibrated bilayer and attached to the selected POPC lipids. The labels were inserted into a bilayer one-by-one, so that after adding of each spin label, unfavorable interatomic contacts were removed by steepest descent energy minimization, and a short MD re-equilibration was performed for 50 ps. An equal number of the labeled lipids were inserted into each leaflet. The prepared system was finally composed of 124 POPC molecules with 4 NBD-PE lipids randomly inserted among the bilayer, corresponding to 4 mol % of bilayer labeling. The system was hydrated with 4217 water molecules (lipid-to-water ratio 1:33). The initial membrane system was equilibrated for 10 ns, and the MD simulations were carried out for 160 ns.

A MD force field of a POPC bilayer was based on the parameters presented by Berger et al. (1997). In POPC and NBD-PE lipids, all carbon atoms of CH_2 and CH_3 groups with non-polar hydrogen atoms were treated as united atoms. In the case of NBD-PE, we used the same force field parameters for the glycerol backbone and acyl chains of the PE lipid moiety as those used for an unlabeled POPC lipid molecule. The bond length and angle parameters for the NBD probe were optimized by density functional theory calculations at the UB3LYP/cc-pVDZ level. Partial charges needed for Coulomb interactions were derived from the UB3LYP/cc-pVDZ electron densities by fitting the electrostatic potential to point (ESP) charges. The simple point charge (SPC) model (Hermans et al. 1984) was used for water. MD simulations were carried out at the constant number of particles, constant pressure $P = 1$ atm, and constant temperature $T = 303.15$ K (NPT ensemble). Three-dimensional periodic boundary conditions were applied with the z axis lying along a direction normal to the bilayer. The pressure was controlled semi-isotropically, so that the x–y and z dimensions of the simulation box were allowed to fluctuate independently from each other, keeping the total pressure constant. Thus, during MD simulations, the membrane area and thickness were therefore free to adjust under the NPT condition. The reference temperature and pressure were kept constant using the Berendsen's weak coupling scheme (Berendsen et al. 1984) with a coupling constant of $\tau_T = 0.1$ ps for the temperature

coupling and $\tau_{P(x\ -\ y)} = \tau_{P(z)} = 1.0$ ps for the pressure coupling. Electrostatic interactions were simulated with the particle mesh Ewald (PME) (Darden et al. 1993) approach using a long-range cutoff of 1.4 nm. The cutoff distance of Lennard–Jones interactions was also equal to 1.4 nm. All bond lengths were kept constant using the LINCS routine (Hess et al. 1997). The MD integration time step was 2 fs. The MD simulations were carried out using the GROMACS set of programs, version 4.5.5 (Van Der Spoel et al. 2005). Molecular graphics and visualization were performed using VMD 1.8.6 (Humphrey et al. 1996).

Results and Discussion

Depth-Dependent Fluorescence Quenching

The steady-state and lifetime fluorescence of NBD-PE incorporated into POPC lipid vesicles were examined in the absence and in the presence of spin-labeled lipids. To probe specific depths within a membrane, a series of six different spin probes was used, in which either Tempo or Doxyl spin quenchers are covalently attached to a phospholipid molecule (Fig. 1a). NBD-PE and the lipid-attached spin quenchers were incorporated into POPC lipid vesicles by co-extrusion. The concentration of 1 mol % NBD-PE was constant, while the molar fraction of each spin quencher was gradually varied from 0 to 0.3, respectively. Fluorescence spectra and lifetime decays of NBD-PE measured in the absence and in the presence of two spin-labeled probes, namely, Tempo-PC and 12-Doxyl-PC, are shown in Fig. 1b–e. The spin moiety of these probes is known to reside at shallow and deep locations within a membrane (Kyrychenko and Ladokhin 2013), so that they are expected to quench the headgroup-attached NBD fluorophore of NBD-PE to different degrees. Figure 1b–e shows that, in the case of both Tempo-PC and 12-Doxyl-PC, the gradual increase in the concentration of the quenchers results in the systematic decrease in steady-state intensity, which is also accompanied by lifetime shortening of the NBD fluorescence. At any given concentration of the quenchers, the quenching efficiency measured by both intensity and lifetime was found to be stronger for Tempo-PC as compared to those of 12-Doxyl-PC. To explore lifetime shortening of NBD due to the depth-specific quenching in a quantitative way, we subjected all the decay curves to deconvolution analysis. It has been reported previously that an NBD probe attached to lipids or proteins reveals multi-exponential fluorescence decays in heterogeneous membrane environment (Posokhov and Ladokhin 2006; Mukherjee et al. 2004; Loura and Ramalho 2007); (Greiner et al. 2009). The best fits to all the NBD decays were obtained using a sum of two exponentials. In quantitative analysis, we used amplitude-weighted average lifetimes (τ_α) calculated as described previously (Posokhov and Ladokhin 2006).

Figure 1b and d shows that in the presence of 30 mol % of Tempo-PC and 12-Doxyl-PC in LUVs, the normalized fluorescence intensity of NBD-PE was decreased from 1.0 up to 0.36 and 0.57, respectively. In accordance with this decrease, the lifetime of NBD-PE was also shortened from 5.37 ns up to 2.86 and 3.25 ns, as shown in Fig. 1c, e.

Stern–Volmer Analysis

In order to determine the static and dynamic contributions to NBD-PE quenching by a series of depth-specific quenchers, we calculated the ratios of both the fluorescence intensities ($F_0/F - 1$) and lifetimes ($\tau_0/\tau - 1$). Figure 2 shows examples of plots of $F_0/F - 1$ and $\tau_0/\tau - 1$ on the mole fraction of Tempo-PC and 12-Doxyl-PC quenchers in POPC bilayers. Applying the Stem–Volmer equation allows us to derive the apparent Stem–Volmer quenching constant, K_{SV}. As shown in Fig. 2, the ratios of steady-state intensities and lifetimes differ significantly for these two quenchers at all mole fractions. The total Stern–Volmer quenching constant K_{SV}(total), measured in a steady-state fluorescence quenching experiment, contains contributions from both "static" and "dynamic" quenching: $K_{SV}(\text{total}) = K(\text{static}) + K_{SV}(\text{dynamic})$. Measuring lifetime quenching allows one to extract a pure "dynamic" quenching component K_{SV}(dynamic) and to calculate $K(\text{static}) = K_{SV}(\text{total}) - K_{SV}(\text{dynamic})$. As can be noted from Table 1, in the case of the shallow Tempo-PC, the "static" and "dynamic" components contribute almost equally to the "total" quenching ($K_{SV}(\text{dynamic}) = 2.8$ 1/M; $K(\text{static}) = 5.8 - 2.8 = 3.0$ 1/M). In contrast, for the deep 12-Doxyl-PC probe, the overall quenching is dominated by the dynamic mechanism ($K_{SV}(\text{dynamic}) = 2.2$ 1/M; $K(\text{static}) = 2.6 - 2.2 = 0.4$ 1/M).

Our findings point out that the assumption of a purely static quenching mechanism for calculating depth from steady-state fluorescence quenching has some limitations for long-lifetime fluorophores because of thermal motions in the lipid membrane occurring during the excited-state lifetime. While this is still a reasonable approximation when fluorophores with short lifetimes are used, the same may not be true for probes with long-lived excited states, such as NBD, pyrene (Sassaroli et al. 1995), and anthracene (Chattopadhyay and Mukherjee 1999a; Haldar et al. 2012). Our recent MD simulations of a series of spin-labeled lipids in a POPC bilayer have shown that the diffusive reorientational dynamics of the spin groups occurs on a nanosecond time scale and depends strongly on their depths within the membrane (Kyrychenko and Ladokhin 2013). The rotational times decrease rapidly from 10 ns for

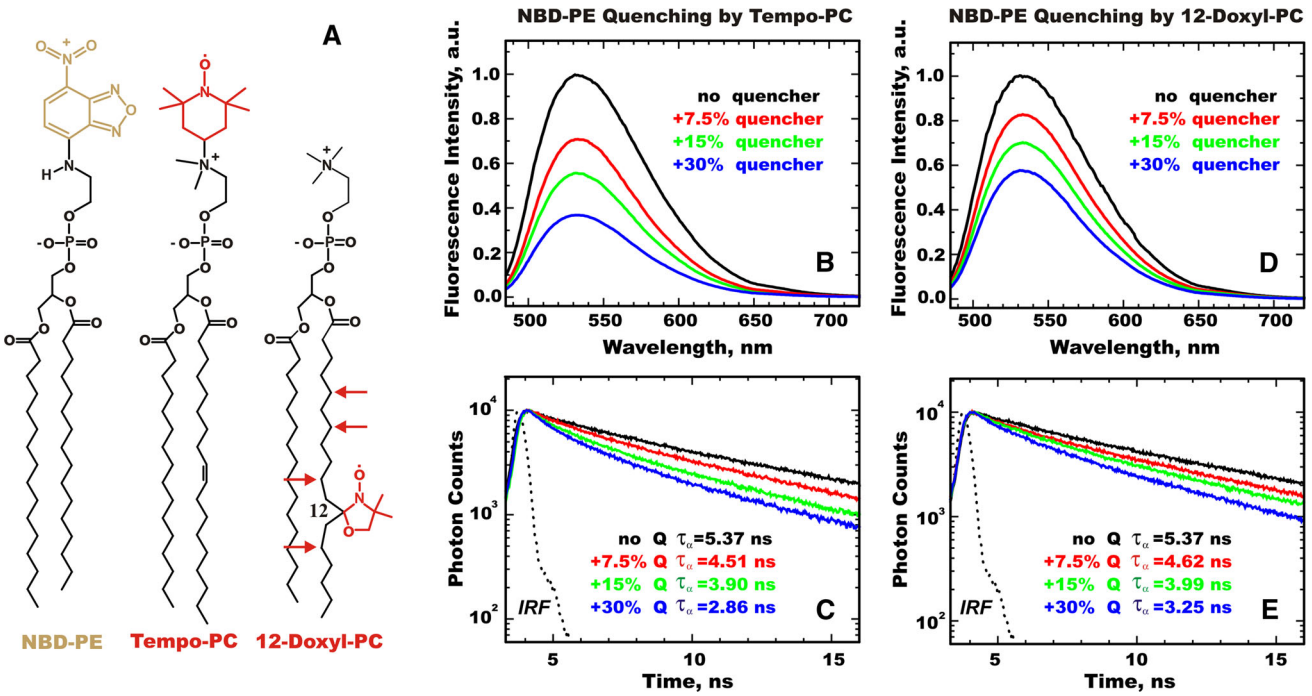

Fig. 1 Depth-dependent fluorescence quenching of NBD-PE by spin-labeled lipids. **a** Molecular structure of NBD-PE (1,2-dipalmitoyl-*sn*-glycero-3-phosphoethanolamine-*N*-(7-nitro-2-1,3-benzoxadiazol-4-yl), Tempo-PC (1-palmitoyl-2-oleoyl-*sn*-glycero-3-phospho-(TEMPO)-choline), and 12-Doxyl-PC (1-palmitoyl-2-stearoyl-(*12*-doxyl)-*sn*-glycero-3-phosphocholine) lipids. Tempo and Doxyl spin labels are shown in *red*. Attachment positions of a doxyl moiety along the *sn*-2 acyl chain of the host lipid are indicated by *red arrows*. **b**–**e** Example of depth-dependent fluorescence quenching of NBD-PE by Tempo-PC (**b**, **c**) and 12-Doxyl-PC (**d**, **e**) measured using steady-state and time-resolved fluorescence methods. Increasing the spin label concentration in lipid vesicles resulted in reduction of the fluorescence intensity of the NBD emission (**b**, **d**) and shortening of its excited-state lifetime (**c**, **e**) (Color figure online)

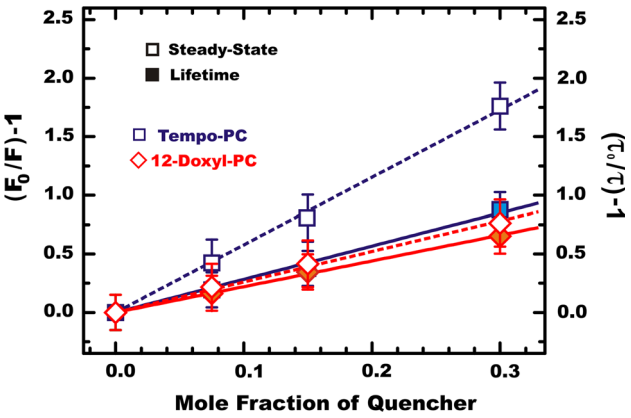

Fig. 2 Examples of Stern–Volmer plots of fluorescence quenching of NBD-PE incorporated into lipid vesicles composed of various mixtures of POPC and either Tempo-PC or 12-Doxyl-PC quenchers. The lines represent the best fit to the steady-state intensity (*open squares* and *dotted lines*) and lifetime (*solid squares* and *solid lines*) data using the Stern–Volmer equation

the headgroup-attached Tempo moiety up to 2.3 ns for the deeply located 14-Doxyl group, indicating a progressive increase in the degree of mobility of the spin group. The excited-state lifetime of the NBD-PE fluorophore in the lipid vesicles is about 5.4 ns, so that the spin moiety attached to the lipid headgroup (Tempo-PC) and the upper part of the lipid acyl tail (5-Doxyl and 7-Doxyl) remain relatively rigidly fixed by the membrane environment on this time scale, leading to the large contributions of the static quenching. In contrast, the almost pure dynamic quenching of the NBD fluorophore by the deeper probes 12-Doxyl and 14-Doxyl could be explained by their shorter relaxation times, characterizing the increase in overall lipid internal motions down to the bilayer center.

Depth of NBD Fluorophore

The distribution analysis (DA) methodology (Ladokhin 1997, 2014) approximates the transverse quenching profile (QP) of a fluorophore with a Gaussian function (Eq. 1):

$$QP(h) = G(h) + G(-h) = \frac{s}{\sigma\sqrt{2\pi}}\exp\left[-\frac{(h-h_{\mathrm{m}})^2}{2\sigma^2}\right] + \frac{s}{\sigma\sqrt{2\pi}}\exp\left[-\frac{(h+h_m)^2}{2\sigma^2}\right] \quad (1)$$

In the case of analyzing deeply penetrating fluorophores, a symmetrical second Gaussian is added to account for

Table 1 Steady-state and lifetime quenching of NBD-PE containing varying molar fractions of spin-labeled quenchers in POPC lipid vesicles

Quencher	Steady-state quenching[a] $(F_0/F)-1$				Lifetime quenching[a] $(\tau_0/\tau)-1$			
	Molar fraction of quenchers			K_{SV}[b]	Molar fraction of quenchers			K_{SV}[b]
	0.075	0.15	0.30		0.075	0.15	0.30	
Tempo-PC	0.423	0.805	1.762	5.8	0.193	0.377	0.878	2.8
5-Doxyl-PC	0.462	0.909	2.176	7.0	0.294	0.539	1.148	3.8
7-Doxyl-PC	0.370	0.791	1.678	5.5	0.160	0.444	0.982	3.2
10-Doxyl-PC	0.352	0.731	1.450	4.8	0.155	0.436	0.925	3.0
12-Doxyl-PC	0.216	0.415	0.763	2.6	0.152	0.346	0.652	2.2
14-Doxyl-PC	0.202	0.346	0.681	2.3	0.135	0.303	0.619	2.0

[a] F_0/F and τ_0/τ are the ratios of the fluorescence intensities and amplitude-weighted average lifetimes of 1 mol % NBD-PE incorporated into LUVs in the absence and in the presence of the spin quenchers, respectively. In the absence of the quenchers, the amplitude-weighted average lifetime τ_0 was measured to be 5.37 ns (Fig. 1c, e)

[b] Steady-state and lifetime Stern–Volmer quenching constants for NBD-PE co-incorporated into LUVs containing varying molar fractions of Tempo-PC and *n*-Doxyl-PCs. In the text, the steady-state and lifetime quenching constants are referred to as K_{SV}(total) and K_{SV}(dynamic), respectively

Table 2 MD-estimated immersion depths of the spin labels of Tempo-PC and *n*-Doxyl-PC lipids incorporated into a POPC bilayer (Kyrychenko and Ladokhin 2013)

Spin-labeled lipid	Depth (Å)	Half-width at half-height (Å)
Tempo–PC	18.2	4.8
5–Doxyl–PC	12.1	3.0
7–Doxyl–PC	11.5	3.0
10–Doxyl–PC	10.1	3.8
12–Doxyl–PC	6.4	4.8
14–Doxyl–PC	2.9	4.8

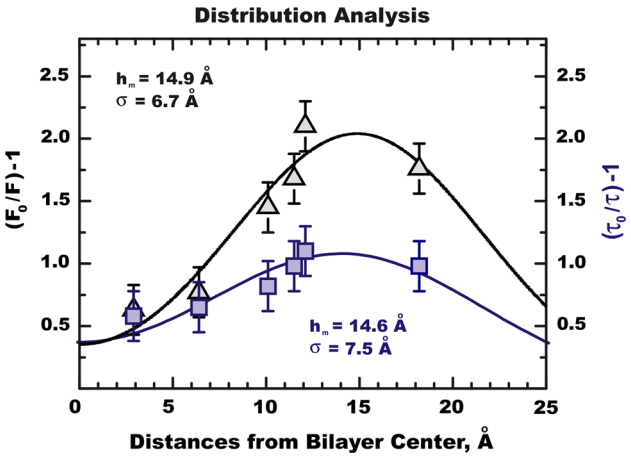

Fig. 3 Distribution analysis of penetration depth of NBD-PE. NBD-PE quenching by spin-labeled lipids embedded in phospholipid vesicles measured using steady-state (*triangles*) and lifetime (*squares*) fluorescence. The spin-labeled lipids were Tempo-PC, 5-, 7-, 10-, 12- and 14-Doxyl-PCs. The immersion depths of their spin groups within the bilayer have been estimated by the MD simulations as given in Table 2. Samples were prepared containing 1 and 30 mol % of NBD-PE and the spin-labeled lipids, respectively. *Solid lines* are the fitting curves of the distribution analysis (Ladokhin 1997, 1999a, 1999b) utilizing Eq. 1. The double-Gaussian fitting parameters h_m and σ represent average position and depth heterogeneity of the NBD group calculated from the bilayer center

trans-leaflet quenching (Ladokhin 1999a). The average positions of the spin quencher calculated from the center of the lipid bilayer have previously been determined by MD simulations of a series of spin-labeled lipids in the model membrane (Table 2).

Application of the DA approach to depth-dependent fluorescence quenching of NBD-PE in LUV is presented in Fig. 3. The NBD fluorophore was found to be located below the membrane interface and its distribution along the bilayer normal is relatively broad, suggesting a high degree of thermal mobility. Due to strong trans-leaflet quenching observed in the middle of the bilayer, the double-Gaussian fitting function was used. Applying DA to steady-state and lifetime quenching data, the membrane depth h_m of the NBD group is found to be 14.9 ± 0.6 Å and 14.6 ± 0.5 Å, respectively.

Previously, fluorescence quenching of NBD-PE by spin-labeled lipids analyzed with the parallax method has indicated an external location of the NBD group, about 14.2 Å from the center of 1,2-dioleyol-*sn*-glycero-3-phosphocholine (DOPC) bilayers (Chattopadhyay and London 1987). Using the same depth-dependent quenching technique, however, a much shallower location of about 18.9 Å has been reported for the same system when another set of spin quenchers was used (Abrams and London 1993); (Kachel et al. 1998). Another study, which also used the parallax method, reported penetration depth of 20.3 Å for the NBD group in NBD-PE (Mukherjee et al. 2004). (Note that our published experimental and computational results demonstrate that the parallax method is prone to substantial systematic errors (Ladokhin 1997,

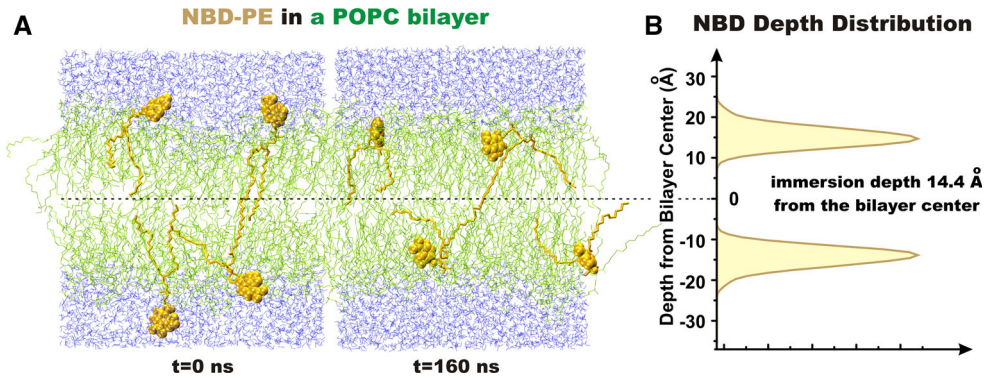

Fig. 4 Distribution of NBD-PE in a bilayer. **a** MD snapshots of the POPC bilayer composed of 124 POPC molecules and four randomly inserted NBD-PE lipids taken at the beginning ($t = 0$ ns) and the end ($t = 160$ ns) of MD sampling. Bilayer shown in stick representations is *olive*, the NBD-PE lipids are *gold*, and water molecules are *blue*. The NBD fluorophore is shown using van der Waals representation. **b** The transverse mass density distribution of the NBD group within the bilayer. The distribution was averaged for the last 70 ns of the MD sampling. The distribution peak position (the depth from the bilayer center) and the half-width are 14.4 and 3.2 Å, respectively (Color figure online)

1999a; London and Ladokhin 2002; Kyrychenko et al. 2013; Ladokhin 2014). In addition, the more external location of the NBD groups found in the later studies could be due to the use of the shallower spin quencher, Tempo-PC. Recently, we have shown that the Tempo group of Tempo-PC lipids incorporated into the bilayer spans a broad region, ranging between 14.4 and 18.2 Å from the bilayer center (Kyrychenko and Ladokhin 2013), which could cause the largest uncertainty in the calculation of the fluorophore depth.

MD Simulations of NBD-PE in a POPC Bilayer

To test and validate our experimental depth-dependent quenching data, we carried out control MD simulations of NBD-PE lipids incorporated into the POPC bilayer. To build an initial configuration, we attached an NBD fluorophore to the choline moiety of lipid molecules, which were randomly selected from the equilibrated POPC bilayer in water (two from both the upper and lower leaflets). In these four lipids, the rest of the phospholipid molecule (the choline moiety and double bond of the oleoyl chain) was modified to transform POPC into NBD-PE.

Figure 4a shows two MD simulation snapshots of the NBD-PE lipids incorporated in the POPC bilayer taken at the beginning ($t = 0$ ns) and the end ($t = 160$ ns) of the MD sampling. At $t = 0$ ns, the NBD groups of all four NBD-PE lipids were faced toward bulk water, Fig. 4a. During MD simulations, all were gradually moved from bulk water deeper into the bilayer interface. The average immersion depth of the NBD moiety was calculated from transverse mass density distributions and found to be 14.4 Å, as shown in Fig. 4b.

The earlier MD simulations of NBD-chain-labeled phosphatidylcholine (NBD-PC) inserted into the fluid phase DPPC bilayer have revealed that despite covalent attachment to the acyl chain, the NBD fluorophore could loop to the transverse location closer to the interface (Loura and Ramalho 2007); (Loura et al. 2008). The simulations have demonstrated that due to the chromophore polarity and the acyl chain flexibility, the NBD moieties in both C6-NBD-PC and C12-NBD-PC derivatives were found to move to the water–lipid interface, favoring residence at 13.1 and 13.8 Å from the bilayer center (Loura and Ramalho 2007). Recently, NBD-labeled fatty amines, possessing varying alkyl chain length, NBD-C_n (where n varied from 4 to 12), have been simulated in a POPC bilayer (Filipe et al. 2011). For all NBD derivatives inserted in the bilayer, the equilibrium location of the NBD fluorophore was found to be at 14–14.5 Å from the bilayer center. Thus, the previous MD studies agree overall that when the NBD group is attached to either the long hydrocarbon chain or the headgroup of the host molecule, it predominantly occupies a location within the bilayer shallower than that which would be expected solely from the chemical structure of the fluorescent probe molecule. These findings also correlate with the transverse location of the NBD group in NBD-PE at 14.4 Å from the center of the POPC bilayer, as revealed by our MD simulations.

Depth-Dependent Overlaps between NBD and Spin Quenchers

We have recently shown that the overlaps between the transverse distributions of a fluorophore and quenchers could be used to reconstruct the depth-dependent fluorescence quenching profile in membranes (Kyrychenko et al. 2013). Such a simplified approach assumes that the quenching of the fluorophore is proportional to the fluorophore-to-quencher distribution overlap, so that the most

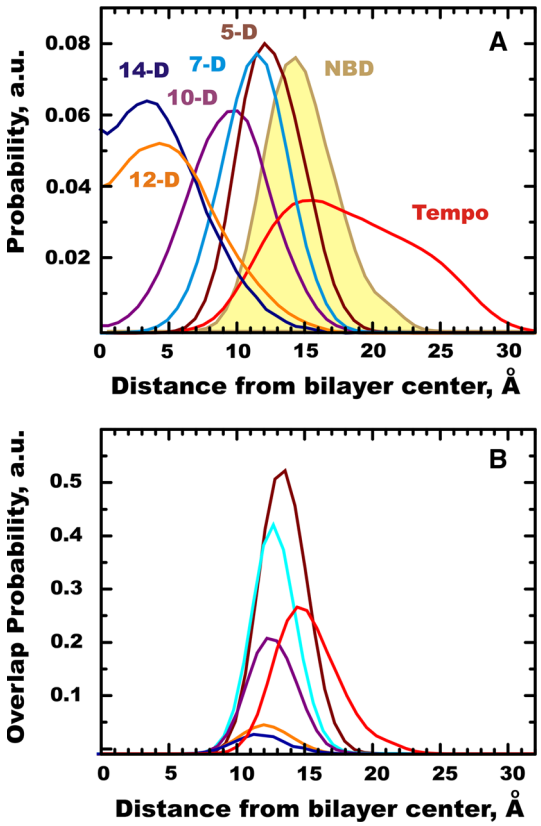

Fig. 5 MD-simulated depth probability profiles. **a** Transverse depth distribution of the NBD fluorophore and the spin probes (Tempo and Doxyl referred to as 5-D, 7-D, 10-D, 12-D, and 14-D for *n*-Doxyl-PCs where $n = 5$, 7, 10, 12, 14, respectively) taken from Fig. 4 and ref (Kyrychenko and Ladokhin 2013). **b** The most efficient quenching will occur when NBD and spin quenchers are both located at the same depth within a membrane, which could be quantitatively estimated by their overlap areas. These overlap areas correlate well with experimental depth-dependent quenching of NBD-PE by spin-labeled lipids in a bilayer

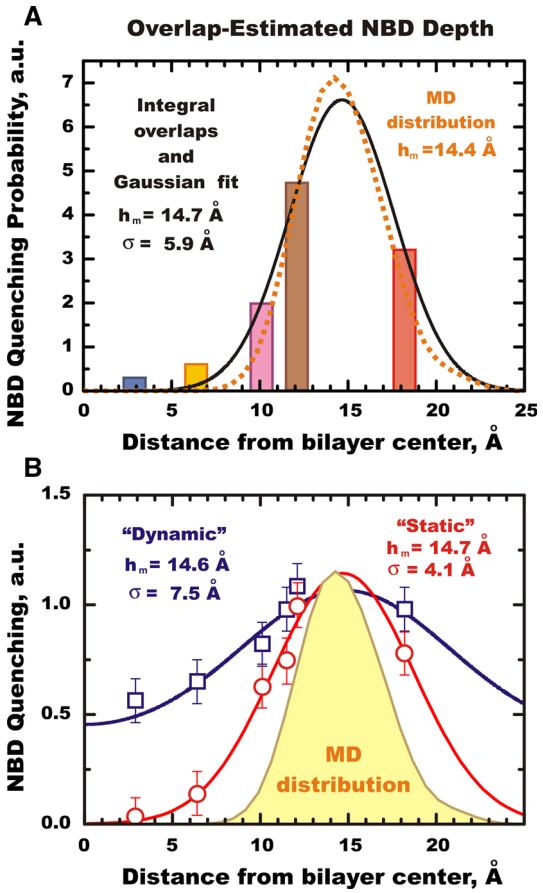

Fig. 6 Overlap-estimated depth compared to direct MD simulation. **a** The depth of the NBD moiety estimated using the overlap quenching integrals of NBD with the particular spin quenchers (integral *bars* color-coded as shown in Fig. 5) is compared with the direct MD simulation of NBD-PE in the bilayer. The overlap integrals were fitted by the Gaussian function with the fitting parameters h_m and σ representing average position and depth heterogeneity of the NBD fluorophore in the lipid bilayer. **b** Depth-dependent profiles plotted for lifetime quenching (*squares*) and "static" quenching (*circles*) calculated as the difference between total and dynamic quenching (*triangles* and *squares* in Fig. 3)

efficient quenching occurs when NBD and spin quenchers are both located at the same depth within a membrane. Figure 5a shows the transverse distribution of NBD and those of Tempo and a series of *n*-Doxyl spin probes (data taken from (Kyrychenko and Ladokhin 2013)). To normalize the occurrence probability of NBD and the various spin probes within a membrane, an area under each profile was normalized to 100 %. The probability of NBD being quenched by the particular spin quencher was estimated by calculating the overlap of their transverse distributions as shown in Fig. 5b. The overlap areas correlate well with the experimental depth-dependent quenching of NBD-PE measured using the spin-labeled lipids in LUV (Table 1). The overlap areas between NBD and the spin probes decrease in the order 5-D > 7-D ≈ Tempo > 10-D > 12-D > 14-D.

To calculate the quantitative quenching probability, the overlap areas were integrated and plotted against the MD-estimated depth of the spin quenchers (Table 2) as shown in Fig. 6a. Using the distribution analysis method, the depth of the NBD moiety was estimated by fitting the overlap integrals to the three-parameter Gaussian function, Eq. 1. The DA yields an immersion depth of $h_m = 14.7$ Å, which is in good agreement with the peak position of 14.4 Å of the NBD distribution derived by direct MD simulations of NBD-PE in the POPC bilayer. This value also agrees perfectly with the experimental depth of the NBD group measured for NBD-PE in LUVs (Fig. 3).

We have recently developed an approach for refining immersion depths via extracting "static" depth profiles by utilizing a combination of steady-state and time-resolved depth-dependent fluorescence quenching (Kyrychenko and Ladokhin 2014). Figure 6b shows that the calculated

"static" quenching profile became narrowed compared to the "dynamic" one, due to elimination of thermal motions of the NBD group in membranes occurring during its excited-state lifetime. Figure 6b also demonstrates that the "static" profile is characterized by $h_m = 14.7$ Å, and it agrees well with the MD-estimated distribution of NBD in membranes.

Application of DA to Fluorescence Quenching of Diphtheria Toxin T-Domain

In past years, we have used a series of NBD-labeled single-cysteine mutants of the T-domain of diphtheria toxin to study its acid-induced binding and insertion into lipid membranes (Ladokhin et al. 2004), (Kyrychenko et al. 2009; Rodnin et al. 2008, 2010). The T-domain has two hydrophobic α-helices TH8 and TH9, which form a transmembrane hairpin. Here, we illustrate the application of the DA methodology by examining steady-state and time-resolved depth-dependent quenching of NBD-labeled mutants N366C and P378C. According to the X-ray structure of the soluble T-domain (Bennett and Eisenberg 1994), these labels will be positioned in the middle and at the end of the TH9 helix. According to our previous LysoUB topology measurements (Kyrychenko et al. 2009), this helix adopts a transmembrane conformation in the inserted form, which is expected to place the probe attached at position 366 close to the bilayer center, and the one attached at position 378 close to the interface. In both cases, the T-domain samples carrying mutations were tested to maintain normal binding to lipid vesicles and the normal ability to insert into lipid vesicles, as verified by the blue shift in its native tryptophan fluorescence upon association with lipid vesicles at low pH.

The membrane depth of the NBD probe attached at positions 366 and 378 was examined by depth-dependent fluorescence quenching. The steady-state and time-resolved quenching were measured for the samples containing 1 μM of the labeled protein and 1 mM of LUV composed of POPC:POPG in the ratio of 3:1 + 30 mol % of spin-labeled lipids after 2 h incubation in 50 mM phosphate buffer at pH 4.5. To determine the transverse

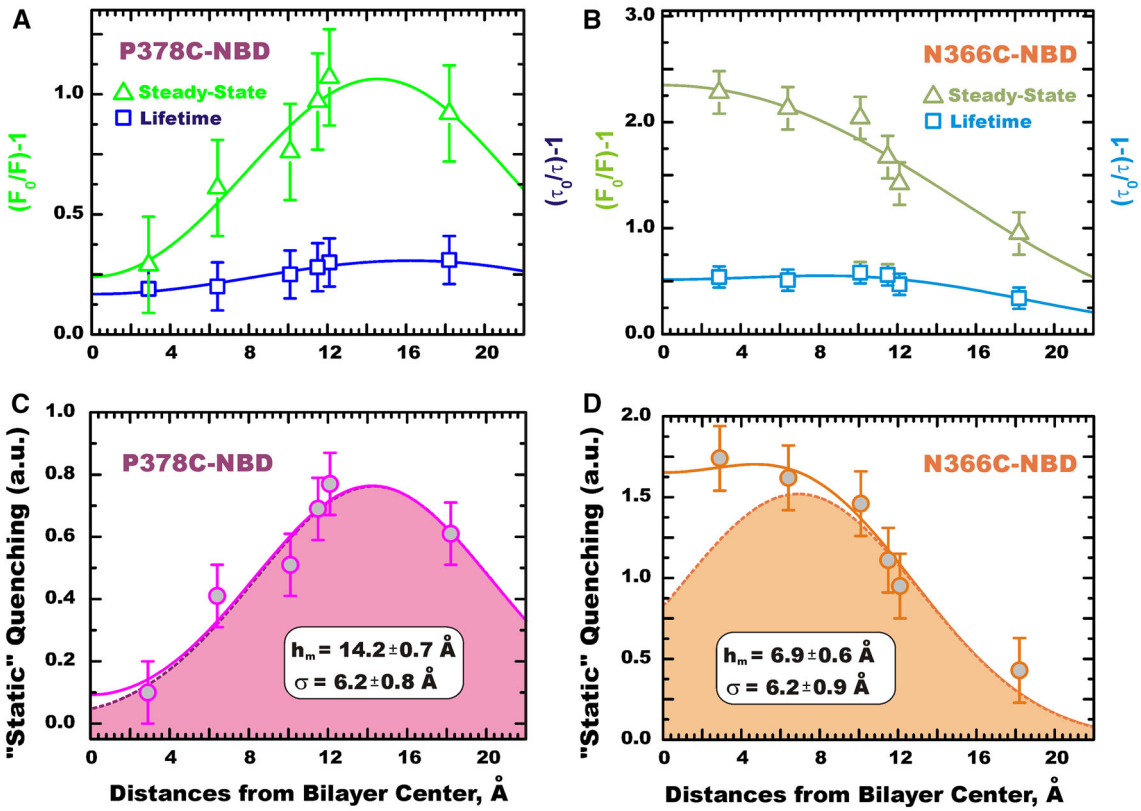

Fig. 7 Fluorescence quenching of NBD-labeled T-domain. Distribution analysis of depth-dependent fluorescence quenching profiles of P378C-NBD and N366C-NBD mutants of the T-domain obtained with a series of the spin-labeled lipids (Tempo-PC and *n*-Doxyl–PCs with $n = 5, 7, 10, 12$, and 14). Panels **a**–**b** show application of the DA methodology to steady-state ("total" quenching, *open triangles*) and lifetime ("dynamic" quenching, *open squares*) fluorescence quenching and "static" quenching. (**c**–**d**) A deconvolution of the "static" fluorescence quenching (*filled circles*) was calculated as the difference between total quenching and dynamic profiles (Kyrychenko and Ladokhin 2014). The single Gaussian depth distributions are shown as *shaded profiles*

position of the NBD probe in the lipid bilayer, we constructed depth-dependent quenching profiles where steady-state and lifetime quenching efficiencies $(F_0/F)-1$ and $(\tau_0/\tau)-1$ are plotted against the depth of the spin quenchers (Fig. 7a, b). Quantitative information on membrane penetration of NBD was extracted from these depth-dependent quenching data using the distribution analysis (DA) methodology. Solid lines in Fig. 7a, b show that the steady-state and lifetime quenching could be well fitted by a pair of mirror-symmetric Gaussian functions (one for each leaflet, Eq. 1) to take into account transverse distributions of lipid and protein moieties originating from the thermal motion in the bilayer. In addition, to reduce the quenching contribution from the transverse diffusion of a probe occurring during the excited-state lifetime, we deconvoluted pure "static" quenching by subtracting the "dynamic" lifetime quenching component from the total steady-state quenching (Kyrychenko and Ladokhin 2014). Figure 7c, d shows that this procedure leads to narrower, better-defined quenching profiles for the NBD probe compared with those obtained by traditional steady-state quenching experiments. The NBD fluorophores attached at positions 378 and 366 were found to be at depths of about 14.5 and 6.9 Å from the bilayer center, which indeed corresponds to the expectation for the transmembrane conformation of TH9.

Summary

In this study, we present a refinement of the methodology for determining membrane penetration via a combination of fluorescence spectroscopy and MD simulations using dye-labeled lipid, NBD-PE, as a model. We utilize steady-state and time-resolved depth-dependent fluorescence quenching of NBD with six different spin-labeled lipids with a quencher position varying systematically along a phospholipid molecule ranging from the lipid headgroup (Tempo-PC, in which a nitroxide Tempo probe is attached to a choline moiety of phospholipid) to acyl chain methylene carbons (*n*-Doxyl-PC, in which Doxyl moiety is covalently introduced to *n*-th carbon atoms of *sn*-2 acyl chain with $n = 5, 7, 10, 12$, and 14, respectively) (Fig. 1a). In order to more accurately define the position of the spin quencher groups of Tempo-PC and *n*-Doxyl-PCs within the membrane, we utilized our refined depth scale that was recently derived by direct molecular dynamics (MD) simulations of a series of spin-labeled lipids in the model membrane (Kyrychenko and Ladokhin 2013).

Using the Distribution Analysis (DA) method (Ladokhin 1997, 2014), the immersion depth of the NBD fluorophore was estimated to be at $h_m = 14.7$ Å from the bilayer center. In addition to experimental quenching data, we validated the DA results by MD simulations of the depth distribution of the NBD fluorophore of NBD-PE incorporated into the POPC bilayer: the depth and the distribution half-width of the NBD moiety were determined to be 14.4 and 3.2 Å, respectively. Moreover, we demonstrated that the quenching profile of the NBD probe in the bilayer could be alternatively derived by estimating area overlaps between the MD-estimated depth distributions of NBD and each of the spin quenchers, calculated previously (Kyrychenko and Ladokhin 2013). Finally, we illustrated the application of the DA methodology by determining membrane penetration of site selectively labeled mutants of diphtheria toxin T-domain, confirming the transmembrane conformation of TH9 helix in its membrane-inserted form.

Acknowledgments This work was performed using computational facilities of the joint computational cluster of SSI "Institute for Single Crystals" and Institute for Scintillation Materials of National Academy of Science of Ukraine incorporated into Ukrainian National Grid. This research was supported by National Institutes of Health Grant GM-069783 (A.S.L.). A.K. also acknowledges support of Grant 0113U002426 of Ministry of Education and Science of Ukraine.

References

Abrams FS, London E (1993) Extension of the parallax analysis of membrane penetration depth to the polar region of model membranes: use of fluorescence quenching by a spin-label attached to the phospholipid polar headgroup. Biochemistry 32:10826–10831

Armstrong VT, Brzustowicz MR, Wassall SR, Jenski LJ, Stillwell W (2003) Rapid flip-flop in polyunsaturated (docosahexaenoate) phospholipid membranes. Arch Biochem Biophys 414:74–82

Bartlett GR (1959) Phosphorus assay in column chromatography. J Biol Chem 234:466–468

Bennett MJ, Eisenberg D (1994) Refined structure of monomelic diphtheria toxin at 2.3 Å resolution. Protein Sci 3:1464–1475

Berendsen HJC, Postma JPM, van Gunsteren WF, DiNola A, Haak JR (1984) Molecular dynamics with coupling to an external bath. J Chem Phys 81:3684–3690

Berger O, Edholm O, Jähnig F (1997) Molecular dynamics simulations of a fluid bilayer of dipalmitoylphosphatidylcholine at full hydration, constant pressure, and constant temperature. Biophys J 72:2002–2013

Chattopadhyay A, London E (1987) Parallax method for direct measurement of membrane penetration depth utilizing fluorescence quenching by spin-labeled phospholipids. Biochemistry 26:39–45

Chattopadhyay A, London E (1988) Spectroscopic and ionization properties of *N*-(7-nitrobenz-2-oxa-1,3-diazol-4-yl)-labeledlipid-sinmodelmembranes. Biochim Biophys Acta 938:24–34

Chattopadhyay A, Mukherjee S (1999a) Depth-dependent solvent relaxation in membranes: wavelength-selective fluorescence as a membrane dipstick. Langmuir 15:2142–2148

Chattopadhyay A, Mukherjee S (1999b) Red edge excitation shift of a deeply embedded membrane probe: implications in water penetration in the bilayer. J Phys Chem B 103:8180–8185

Darden T, York D, Pedersen L (1993) Particle mesh Ewald: an N × log(N) method for Ewald sums in large systems. J Chem Phys 98:10089–10092

Feigenson GW (1997) Partitioning of a fluorescent phospholipid between fluid bilayers: dependence on host lipid acyl chains. Biophys J 73:3112–3121

Filipe HAL, Moreno MJ, Loura LMS (2011) Interaction of 7-nitrobenz-2-oxa-1,3-diazol-4-yl-labeled fatty amines with 1-palmitoyl, 2-oleoyl-*sn*-glycero-3-phosphocholine bilayers: a molecular dynamics study. J Phys Chem B 115:10109–10119

Greiner AJ, Pillman HA, Worden RM, Blanchard GJ, Ofoli RY (2009) Effect of hydrogen bonding on the rotational and translational dynamics of a headgroup-bound chromophore in bilayer lipid membranes. J Phys Chem B 113:13263–13268

Haldar S, Kombrabail M, Krishnamoorthy G, Chattopadhyay A (2012) Depth-dependent heterogeneity in membranes by fluorescence lifetime distribution analysis. J Phys Chem Lett 3:2676–2681

Hermans J, Berendsen HJC, Van Gunsteren WF, Postma JPM (1984) A consistent empirical potential for water–protein interactions. Biopolymers 23:1513–1518

Hess B, Bekker H, Berendsen HJC, Fraaije JGEM (1997) LINCS: a linear constraint solver for molecular simulations. J Comput Chem 18:1463–1472

Humphrey W, Dalke A, Schulten K (1996) VMD: visual molecular dynamics. J Mol Graph 14:33–38

Huster D, Müller P, Arnold K, Herrmann A (2003) Dynamics of lipid chain attached fluorophore 7-nitrobenz-2-oxa-1,3-diazol-4-yl (NBD) in negatively charged membranes determined by NMR spectroscopy. Eur Biophys J 32:47–54

Kaback HR, Wu J (1999) What to do while awaiting crystals of a membrane transport protein and thereafter. Acc Chem Res 32:805–813

Kachel K, Asuncion-Punzalan E, London E (1998) The location of fluorescence probes with charged groups in model membranes. Biochim Biophys Acta 1374:63–76

Kyrychenko A (2010) A molecular dynamics model of rhodamine-labeled phospholipid incorporated into a lipid bilayer. Chem Phys Lett 485:95–99

Kyrychenko A, Ladokhin AS (2013) Molecular dynamics simulations of depth distribution of spin-labeled phospholipids within lipid bilayer. J Phys Chem B 117:5875–5885

Kyrychenko A, Ladokhin AS (2014) Refining membrane penetration by a combination of steady-state and time-resolved depth-dependent fluorescence quenching. Anal Biochem 446:19–21

Kyrychenko A, Posokhov YO, Rodnin MV, Ladokhin AS (2009) Kinetic intermediate reveals staggered pH-dependent transitions along the membrane insertion pathway of the diphtheria toxin T-domain. Biochemistry 48:7584–7594

Kyrychenko A, Wu F, Thummel RP, Waluk J, Ladokhin AS (2010) Partitioning and localization of environment-sensitive 2-(2′-pyridyl)- and 2-(2′-pyrimidyl)-indoles in lipid membranes: a joint refinement using fluorescence measurements and molecular dynamics simulations. J Phys Chem B 114:13574–13584

Kyrychenko A, Sevriukov IY, Syzova ZA, Ladokhin AS, Doroshenko AO (2011) Partitioning of 2,6-bis(1H-benzimidazol-2-yl)pyridine fluorophore into a phospholipid bilayer: complementary use of fluorescence quenching studies and molecular dynamics simulations. Biophys Chem 154:8–17

Kyrychenko A, Tobias DJ, Ladokhin AS (2013) Validation of depth-dependent fluorescence quenching in membranes by molecular dynamics simulation of tryptophan octyl ester in POPC bilayer. J Phys Chem B 117:4770–4778

Ladokhin AS (1997) Distribution analysis of depth-dependent fluorescence quenching in membranes: a practical guide. In: Ludwig Brand MLJ (ed) Methods in Enzymology, vol 278. Academic Press, New York, pp 462–473

Ladokhin AS (1999a) Analysis of protein and peptide penetration into membranes by depth-dependent fluorescence quenching: theoretical considerations. Biophys J 76:946–955

Ladokhin AS (1999b) Evaluation of lipid exposure of tryptophan residues in membrane peptides and proteins. Anal Biochem 276:65–71

Ladokhin AS (2014) Measuring membrane penetration with depth-dependent fluorescence quenching: distribution analysis is coming of age. Biochim Biophys Acta 1838:2289–2295

Ladokhin AS, Legmann R, Collier RJ, White SH (2004) Reversible refolding of the diphtheria toxin T-domain on lipid membranes. Biochemistry 43:7451–7458

London E, Ladokhin AS (2002) Measuring the depth of amino acid residues in membrane-inserted peptides by fluorescence quenching. Curr Top Membr 52:89–115

Loura LMS (2012) Lateral distribution of NBD-PC fluorescent lipid analogs in membranes probed by molecular dynamics-assisted analysis of Förster Resonance Energy Transfer (FRET) and fluorescence quenching. Int J Mol Sci 13:14545–14564

Loura LMS, Prates Ramalho JP (2011) Recent developments in molecular dynamics simulations of fluorescent membrane probes. Molecules 16:5437–5452

Loura LMS, Ramalho JPP (2007) Location and dynamics of acyl chain NBD-labeled phosphatidylcholine (NBD-PC) in DPPC bilayers. A molecular dynamics and time-resolved fluorescence anisotropy study. Biochim Biophys Acta 1768:467–478

Loura LMS, Fernandes F, Fernandes AC, Ramalho JPP (2008) Effects of fluorescent probe NBD-PC on the structure, dynamics and phase transition of DPPC. A molecular dynamics and differential scanning calorimetry study. Biochim Biophys Acta 1778:491–501

Mayer LD, Hope MJ, Cullis PR (1986) Vesicles of variable sizes produced by a rapid extrusion procedure. Biochim Biophys Acta 858:161–168

Mazères S, Schram V, Tocanne JF, Lopez A (1996) 7-nitrobenz-2-oxa-1,3-diazole-4-yl-labeled phospholipids in lipid membranes: differences in fluorescence behavior. Biophys J 71:327–335

Mukherjee S, Raghuraman H, Dasgupta S, Chattopadhyay A (2004) Organization and dynamics of *N*-(7-nitrobenz-2-oxa-1,3-diazol-4-yl)-labeled lipids: a fluorescence approach. Chem Phys Lipids 127:91–101

Posokhov YO, Ladokhin AS (2006) Lifetime fluorescence method for determining membrane topology of proteins. Anal Biochem 348:87–93

Pucadyil TJ, Mukherjee S, Chattopadhyay A (2007) Organization and dynamics of NBD-labeled lipids in membranes analyzed by fluorescence recovery after photobleaching. J Phys Chem B 111:1975–1983

Rodnin MV, Posokhov YO, Contino-Pepin C, Brettmann J, Kyrychenko A, Palchevskyy SS, Pucci B, Ladokhin AS (2008) Interactions of fluorinated Surfactants with diphtheria toxin T-domain: testing new media for studies of membrane proteins. Biophys J 94:4348–4357

Rodnin MV, Kyrychenko A, Kienker P, Sharma O, Posokhov YO, Collier RJ, Finkelstein A, Ladokhin AS (2010) Conformational switching of the diphtheria toxin T domain. J Mol Biol 402:1–7

Sassaroli M, Ruonala M, Virtanen J, Vauhkonen M, Somerharju P (1995) Transversal distribution of acyl-linked pyrene moieties in liquid-crystalline phosphatidylcholine bilayers. A fluorescence quenching study. Biochemistry 34:8843–8851

Shrive JDA, Kanagalingam S, Krull UJ (1996) Influence of structural heterogeneity on the fluorimetric response characteristics of lipid membranes containing nitrobenzoxadiazolyl-dipalmitoyl-phosphatidylethanolamine. Langmuir 12:4921–4928

Skaug MJ, Longo ML, Faller R (2009) Computational studies of Texas Red-1,2-dihexadecanoyl-*sn*-glycero-3-phosphoethanolamine-model building and applications. J Phys Chem B 113:8758–8766

Stubbs CD, Williams BW, Boni LT, Hoek JB, Taraschi TF, Rubin E (1989) On the use of *N*-(7-nitrobenz-2-oxa-1,3-diazol-4-yl)phosphatidylethnolamine in the study of lipid polymorphism. Biochim Biophys Acta 986:89–96

Vaish V, Sanyal S (2011) Non steroidal anti-inflammatory drugs modulate the physicochemical properties of plasma membrane in experimental colorectal cancer: a fluorescence spectroscopic study. Mol Cell Biochem 358:161–171

Van Der Spoel D, Lindahl E, Hess B, Groenhof G, Mark AE, Berendsen HJC (2005) GROMACS: fast, flexible, and free. J Comput Chem 26:1701–1718